Accepted Manuscript

The actinide-platinum binaries Th_3Pt_4 and U_3Pt_4: Crystallographic investigation and heavy-fermion behavior of the ferromagnetically ordered U_3Pt_4

Nicolas Brisset, Grzegorz Chajewski, Alexandre Berche, Mathieu Pasturel, Adam P. Pikul, Olivier Tougait

PII: S0925-8388(17)30668-0

DOI: 10.1016/j.jallcom.2017.02.222

Reference: JALCOM 40950

To appear in: *Journal of Alloys and Compounds*

Received Date: 13 September 2016

Revised Date: 17 February 2017

Accepted Date: 20 February 2017

Please cite this article as: N. Brisset, G. Chajewski, A. Berche, M. Pasturel, A.P. Pikul, O. Tougait, The actinide-platinum binaries Th_3Pt_4 and U_3Pt_4: Crystallographic investigation and heavy-fermion behavior of the ferromagnetically ordered U_3Pt_4, *Journal of Alloys and Compounds* (2017), doi: 10.1016/j.jallcom.2017.02.222.

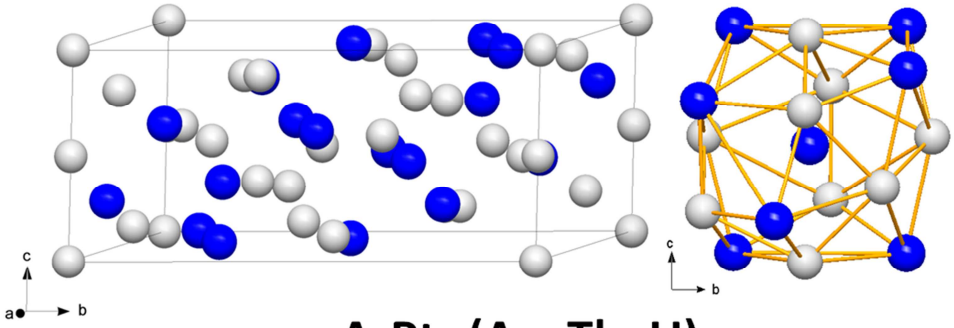

A_3Pt_4 (A = Th, U)

The actinide-platinum binaries Th_3Pt_4 and U_3Pt_4: crystallographic investigation and heavy-fermion behavior of the ferromagnetically ordered U_3Pt_4.

Nicolas Brisset[a], Grzegorz Chajewski[b], Alexandre Berche[a,c], Mathieu Pasturel[a,*], Adam P. Pikul[b], Olivier Tougait[a,d]

[a]*Institut des Sciences Chimiques de Rennes, Chimie du Solide et Matériaux, UMR CNRS 6226, Université Rennes 1, France*

[b]*Institute of Low Temperature and Structural Research, Polish Academy of Sciences, ul. Okólna 2, 50-422, Wrocław, Poland*

[c] *Present address : Institut Charles Gerhard, UMR CNRS 5253, Université Montpellier 2, France*

[d] *Present address : Unité de Catalyse et de Chimie du Solide, UMR CNRS 8181, Université de Lille 1, France*

* corresponding author : mathieu.pasturel@univ-rennes1.fr, tel.: + 33-2-23-23-58-61

Abstract

The existence of the binary compounds Th_3Pt_4 and U_3Pt_4 has been established in the course of the reinvestigation of the U-Pt and Th-Pt systems. Their structural and physical properties have been studied for the first time. Both compounds solidify from the melt of the elemental components with the stoichiometric ratio. Rietveld refinements reveal that they both adopt the trigonal Pu_3Pd_4 structure type ($R\bar{3}$ space group) with lattice parameters at room temperature of a = 13.6870(3) Å, c = 5.7991(2) Å for Th_3Pt_4 and a = 13.2380(2) Å, c = 5.6808(2) Å for U_3Pt_4. Magnetic and specific heat measurements show that Th_3Pt_4 behaves as a typical metal; it was further used as phonon analogue of the U-counterpart. U_3Pt_4 undergoes a ferromagnetic ordering below T_C = 6.5(5) K. Its low temperature specific heat is dominated by an enhanced Sommerfeld coefficient (246(2) mJ mol_U^{-1} K^{-2}) classifying this phase into the heavy fermion family.

Key-words

(A) actinide alloys and compounds ; (C) crystal structure; (C) heat capacity; (D) magnetic measurements

Introduction

The U-Pt binary system has attracted a considerable attention in the last decades, mainly focused on the remarkable coexistence of magnetic ordering and superconductivity in UPt_3 which is still not clearly understood [1] more than thirty years after its recognition [2]. It comprises four intermediate phases, namely UPt, UPt_2, UPt_3 and UPt_5 [3]. Their physical properties were extensively studied.

As stated earlier [4,5] the continuously increasing U-U spacing with platinum content in these binaries provides a favourable playground to understand the phenomena of *5f* electron localization/delocalization in uranium based intermetallics at the origin of the complex physical properties of these compounds. In UPt, where the U-U distances are close to the Hill limit, a ferromagnetic ordering below about 29 K has been confirmed by Prokeš *et al*. [6], while UPt_2 and UPt_5, where the distances are much larger, remain paramagnetic down to the lowest measured temperatures [5]. A literature survey leaves nevertheless some open questions. For example Prokeš *et al*. [7] attribute a low ordering temperature (~ 19 K) of UPt to an impurity phase that cannot be neither uranium nor UPt_2. Similarly an unexplained anomaly has been observed around 5 K in the temperature dependence of the specific heat of UPt [8].

Regarding the Th-Pt system, the phase relations were scarcely studied with a single experimental investigation performed by Thomson in 1964 [9]. The formation of eight Th-Pt intermediate phases is claimed among which only three were structurally characterized (N.B. the novel crystal structure type of $ThPt_2$ was only recently reported by Gumeniuk *et al.* [10]). For the five remaining phases, the author gives their approximate chemical composition, one of them being identified as 'Th_3Pt_4' and forming below about 1873 K from the peritectic Th_3Pt_5 + liquid → Th_3Pt_4 reaction.

Regarding the lack of well established phase relations and characterization of the structural and electronic properties of the A-Pt systems (A = Th, U), we initiated a systematic reinvestigation of these phase diagrams. The present paper focuses on the crystallographic description and physical properties of a novel binary compound, namely U_3Pt_4, discovered in the U-Pt phase diagram, as well as its thorium analogue.

Experimental Methods

The samples were prepared by melting weighted amounts of uranium turnings (99.5 % purity) and platinum wire (99.95 % purity) in a Bühler MAM1 arc-furnace under a residual argon atmosphere. The ingots were turned over and remelted at least twice to ensure homogeneity. The observed weight losses are below the precision of the weighing scale after arc-melting. Heat treatments were performed at various temperatures up to 1723 K for 6 hours by placing the ingot in a cold copper crucible for induction heating (Celes 400 kHz furnace) or at 1173 K for one month in resistance furnaces after enclosing the samples in evacuated silica tubes.

All the samples were examined by scanning electron microscopy (SEM) using a Jeol JSM 7100 F apparatus and the elemental composition of the phases determined by energy dispersive spectroscopy (EDS) performed with an Oxford Instruments SDD X-Max 80mm² detector. The elemental composition is obtained with a 1 at.% error.

Powder X-ray diffraction (XRD) was performed on a Bragg-Brentano θ-2θ geometry Bruker D8 Advance diffractometer working with Cu Kα1 radiation (λ = 1.5406 Å, curved Ge(111) monochromator) and equipped with a fast LynxEye detector. Rietveld refinements of the XRD patterns were undertaken using the Fullprof software [11].

Magnetic properties were measured using a Quantum Design MPMS SQUID magnetometer in the temperature range 1.8–350 K and in applied magnetic fields up to 5 T. Specific heat was measured using a Quantum Design PPMS platform using a thermal relaxation method from room temperature down to 2.0 K.

Results and discussion

A/ Phase formation

SEM-EDS analyses of arc-melted samples with initial composition between those of UPt and UPt_2 reveal the formation of an additional phase with composition 43(1) U – 57(1) Pt in at.%, indicating U_3Pt_4 as a possible chemical formula. The corresponding XRD patterns show the presence of diffraction peaks that could not be indexed with the structural models of UPt and UPt_2, confirming the existence of a new intermediate phase within the U-Pt binary system.

Supplementary SEM-EDS analyses of a sample prepared with the U_3Pt_4 initial composition appeared to be single phased readily from the as-cast state, suggesting a congruent melting. Its XRD pattern was successfully indexed with the trigonal Pu_3Pd_4 structure-type ($R\bar{3}$ space group, no. 148 [12]) with a slight tuning of the lattice parameters. This structural type is adopted by numerous binaries of rare earths (RE) or actinides (A): almost 40 compounds are known with the general formula $(RE,A)_3T_4$ with T = Pd [13], Pt [14], Au [15-18], and RE = *4f* elements (but Pm and Eu) and A = thorium (Th_3Pd_4 [13], Th_3Au_4 [19]).

Regarding the absence of sound characterizations of Th_3Pt_4, new samples were prepared for complementary investigations. Both SEM-EDS and XRD analyses of as-cast ingots with Th_3Pt_4 initial composition confirm the formation of the intermediate phase within the Th-Pt binary phase diagram. The elemental composition was found in agreement with the expected 43(1)Th – 57(1)Pt (in at.%) composition. The sample contains traces of Th_3Pt_5 and ThO_2 that were identified by both SEM-EDS and XRD experiments. A close inspection of the SEM pictures of the as-cast ingots do not reveal any eutectic morphologies indicating that Th_3Pt_4 more likely solidifies by a peritectic reaction involving Th_3Pt_5 as solid phase as previously suggested [9]. The origin of the oxygen contamination was suspected to come from the metallic thorium used for the syntheses. Subsequent heat treatments were found inefficient to remove the secondary phases. The as-cast samples were thus used for crystallographic and physical characterizations.

B/ Structural characterization

The crystal structure of U_3Pt_4 and Th_3Pt_4 was refined by the Rietveld method using the four independent atomic positions of the Pu_3Pd_4–type as starting model. The instrumental peak anisotropy and width were settled using the Thompson-Cox-Hastings pseudo-Voigt profile function parameters obtained on a standard corundum sample. Microabsorption corrections using a Hermann's model developed by Pitschke *et al*. (P_0 = 0, C_P = 1.5265, τ = 0.1454) [20] and preferred orientation using a March's function (G1 = 1.199(4)) [21] were taken into account. Attempts to refine the occupancy rates did not result in significant shifts from full occupancy of the crystallographic sites and these parameters were further fixed to 1. The final least-square fits of the X-ray powder patterns steadily converged to satisfying reliability factors and physically consistent parameters. Figure 1 displays the Rietveld refined plots for XRD patterns of the purest samples. Table 1 gathers the experimental conditions for

the data collections and the structural parameters of the A_3Pt_4 (A = Th, U) phases. Table 2 and Table 3 give the atomic positions along with the thermal displacements parameters and some selected interatomic distances for both phases.

It should be enlightened that the refined Lorentzian enlargement of the peaks enabled to deduce an average crystallite size of 190 Å and 215 Å for U_3Pt_4 and Th_3Pt_4, respectively. This explains the impossibility to find suitable single crystals for XRD data collection. No improvement of the crystallinity was obtained after annealing (1173 K, 7 days or 1773 K, 6h).

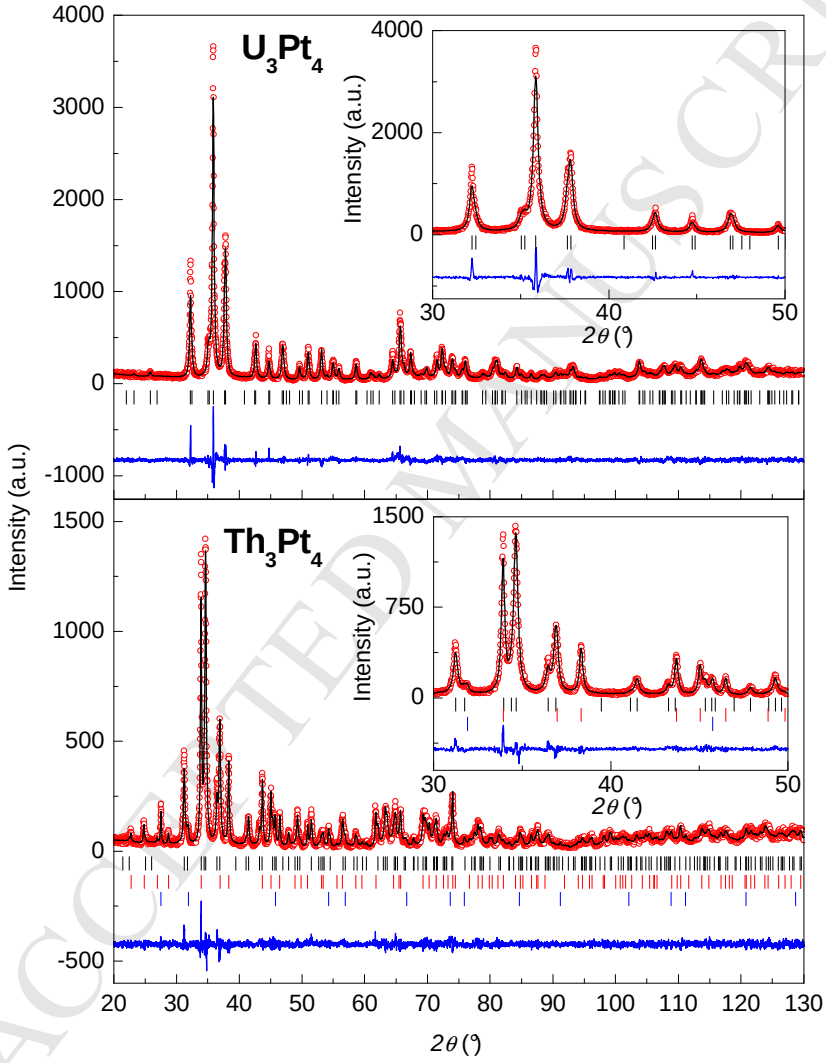

Figure 1. Rietveld refined X-ray diffraction patterns of U_3Pt_4 (upper panel) and Th_3Pt_4 (lower panel). The experimental data (red symbols), the calculated patterns (black line) and the difference between them (blue line) are presented. The vertical ticks represent the refined positions of the diffraction peaks of A_3Pt_4 (A = U, Th; black), Th_3Pt_5 (red) and ThO_2 (blue). The insets show zoomed areas of the main panel.

The refinement confirms the atomic positions from the Pu_3Pd_4 model, *i.e.* a single position for U-atoms in a general *18f* site and 3 independent positions for Pt-atoms in *18f*, *3b* and *3a* sites (fig. 2a). The A-atom coordination sphere is composed of 9 Pt- and 7 A-atoms forming a strongly distorted Frank-Kasper like polyhedron (fig. 2b) often encountered in *5f*-element based intermetallics. The coordination spheres of Pt1 and Pt2 (not shown here) are described in literature whether (i) as 2-face-capped octahedrons by only considering the 8 closest neighbours [22] or (ii) as 14-vertex polyhedra by including the 6 Pt3 at a significantly larger distance [12] (table 3). Similarly, Pt3 is surrounded by 10 [22] or 12 [12] atoms, depending on the selected connectivity limit. Despite including long Pt-ligand distances, the polyhedrons given by Cromer et al. [12] describe a more bounded shell around the platinum atoms. The U-U interatomic distances (table 3) are spread in a rather broad range with 1 U-U distance at 3.398 Å, 2 at 3.703 Å, 2 at 3.929 Å, 2 at 3.934 Å and 2 longer at 4.417 Å, all of them being larger than twice the metallic radius (r_U = 1.56 Å [23]). This is no more the case for Th_3Pt_4 where the shortest Th-Th distance, 3.577 Å, fits well with the sum of its tabulated metallic radius (r_{Th} = 1.798 Å [23]). In addition, very short Th-Pt distances well below the $r_{Th}+r_{Pt}$ = 3.185 Å (with r_{Pt} = 1.387 Å[23]) may illustrate strong covalent character of the bonds. Examination of the interatomic distances of other A-Pt binaries [24] revealed similar trends for all A-A, A-Pt and Pt-Pt contacts. The crystal structure of A_3Pt_4 can thus be described as a 3D network resulting from Pt-Pt and A-Pt bonding.

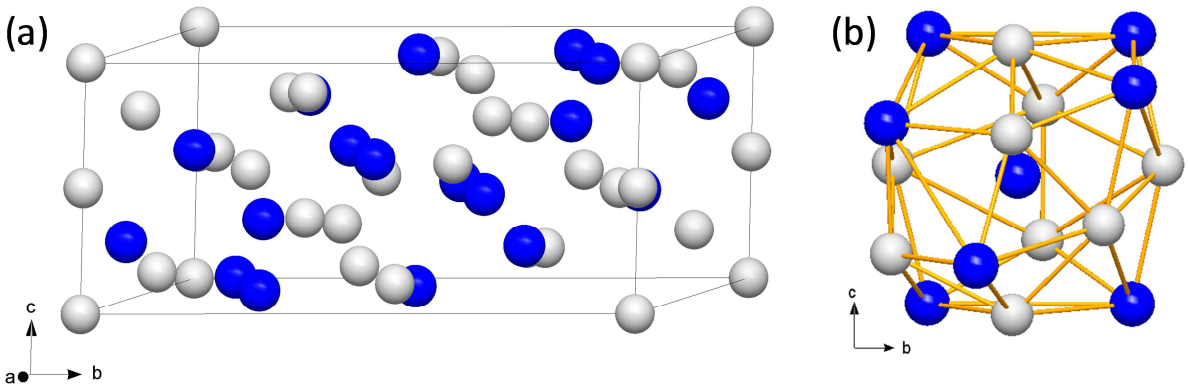

Figure 2. (a) Perspective view of the U_3Pt_4 crystal structure in its hexagonal setting with the U-atoms drawn in blue and the Pt-atoms in grey. (b) Representation of the $[Pt_9U_7]$ coordination polyhedron surrounding the U-atoms.

Table 1. Crystallographic data and Rietveld refinement results for the A_3Pt_4 (A = U, Th) phases.

Formula	U_3Pt_4	Th_3Pt_4
Molecular weight (g mol^{-1})	1494.45	1476.474
Crystal system, Space group	Trigonal, $R\bar{3}$ (n°148)	
Lattice parameters (Å)	a = 13.2380(2) c = 5.6808(2)	a = 13.6870(3) c = 5.7991(2)
Volume ($Å^3$)	862.15(6)	940.83(4)
Z, Density calculated ($g.cm^{-3}$)	6 / 17.271	6 / 15.636
2θ range (°)	10 - 130.30	
2θ Step (°)	0.019707	
Counting time per step (s)	1253	537
Number of reflections	364	387
Number of refined parameters	16	29*
Profile function	Thompson-Cox-Hastings pseudo-Voigt	
Conventional R-factors	R_p = 18.1 R_{wp} = 19.1 χ^2 = 1.67 R_B = 5.10 R_F = 3.29	19.6 21.9 1.26 4.50 3.37

* including scale factor, cell and profile parameters and atomic positions for the Th_3Pt_5 and ThO_2 phases.

Table 2. Refined atomic positions and thermal displacement parameters of A_3Pt_4 (A = Th, U).

Atom	Wyck.	x	y	z	Occupancy	B_{iso}(Å²)
Th	*18f*	0.2093(3)	0.1672(3)	0.2618(7)	1	0.86(6)
Pt3	*18f*	0.0560(4)	0.2759(3)	0.2160(9)	1	0.67(8)
Pt2	*3b*	0	0	½	1	1.2(3)
Pt1	*3a*	0	0	0	1	0.7(2)
U	*18f*	0.2114(2)	0.1656(2)	0.2637(5)	1	0.37(3)
Pt3	*18f*	0.0552(3)	0.2760(2)	0.2222(6)	1	0.51(5)
Pt2	*3b*	0	0	½	1	0.7(2)
Pt1	*3a*	0	0	0	1	0.6(2)

Table 3. Selected interatomic distances (Å) in A_3Pt_4 (A = U, Th).All the standard deviations are less than 0.005 Å.

		U_3Pt_4	Th_3Pt_4
U/Th	-1 Pt3	2.842	2.894
	-1 Pt3	2.874	2.928
	-1 Pt2	2.882	2.966
	-1 Pt1	2.957	3.032
	-1 Pt3	2.996	3.137
	-1 Pt3	3.028	3.139
	-1 Pt3	3.080	3.141
	-1 Pt3	3.152	3.255
	-1 Pt3	3.247	3.367
	-1 U/Th	3.398	3.577
	-2 U/Th	3.703	3.810
	-2 U/Th	3.929	4.013
	-2 U/Th	3.934	4.039
Pt1	-2 Pt2	2.840	2.899
	-6 U/Th	2.957	3.032
	-6 Pt3	3.579	3.679
Pt2	-2 Pt1	2.840	2.899
	-6 U/Th	2.882	2.966
	-6 Pt3	3.702	3.831
Pt3	-1 U/Th	2.842	2.894
	-1 Pt3	2.851	2.928
	-1 U/Th	2.874	2.964
	-2 Pt3	2.929	3.020
	-1 U/Th	2.996	3.137
	-1 U/Th	3.028	3.139
	-1 U/Th	3.080	3.141
	-1 U/Th	3.152	3.255
	-1 U/Th	3.247	3.367
	-1 Pt1	3.579	3.679
	-1 Pt2	3.702	3.831

C/ Magnetic properties

Results of the magnetic measurements performed on an as-cast U_3Pt_4 sample are presented in figure 3. The high temperature (90 - 350 K) paramagnetic domain of the inverse magnetic susceptibility follows a modified Curie-Weiss law:

$$\chi = \chi_0 + \frac{C}{T-\theta_P} \qquad (1)$$

where χ_0 = 3.16(4) 10^{-8} m^3 mol^{-1} represents a sum of temperature independent contributions to the total susceptibility (like *e.g.* core diamagnetism and Pauli paramagnetism of conduction

electrons), $C = 2.31(2)$ m^3 K mol^{-1} is the Curie constant and θ_P = -11.8(6) K is the paramagnetic Curie-Weiss temperature. Since the magnetic susceptibility of Th_3Pt_4 (not shown here) is a few orders of magnitude lower, in agreement with the empty *5f* shell of Th-ions in intermetallics, one can discard the possibility to have magnetic moments carried by platinum atoms, in agreement with previous observations on rare earth based isostructural compounds [25,26]. Therefore one can calculate from the Curie constant the effective magnetic moment μ_{eff} per U-atom, which is equal to $\mu_{eff} = 2.21\ \mu_B$. The obtained value of μ_{eff} is significantly different than those calculated for free U^{3+} and U^{4+} ions (3.62 μ_B and 3.58 μ_B, respectively). This is most probably due to crystal field interactions and strong magnetocrystalline anisotropy usually present in uranium intermetallics (see *e.g.* [27] and [28]) and entirely neglected in the Curie-Weiss fits. Partial delocalization of the *5f*-electrons can be another origin of the reduced value of μ_{eff} and of the moderately enhanced χ_0. θ_P is negative but with a very small absolute value, hence it does not allow to conclude about the predominant ferro- or antiferromagnetic nature of the interactions. Such small positive or negative θ_P values are encountered in the RE_3Pt_4 (RE = Nd, Gd → Tm) ferri- or ferromagnetic series [29] but also in the ferromagnetic superconductors UCoGe and URhGe [30,31].

The anomaly observed in M(T) at low-temperature (fig. 3b) shows that U_3Pt_4 orders magnetically below about 10 K. The Brillouin-like shape of the anomaly as well as bifurcation of the M/H(T) curves indicate a ferromagnetic character of the ordering. A weak magnetic hysteresis visible in M(H) measured at the lowest studied temperature (2 K) and a tendency of M to saturate at high fields (fig. 4c) seems to corroborate the latter hypothesis.

The temperature dependence of the *ac*-susceptibility (fig. 3d) exhibits a distinct anomaly in its real part (χ'). It allows estimating more precisely the Curie temperature of U_3Pt_4 as T_C = 6.5(5) K. The peak in χ'(T) is associated to an anomaly in the imaginary part of the susceptibility (χ''), which is located (as expected) just below T_C. Such a feature shows energy losses caused by alternate probing magnetic field and is characteristic of ferromagnets. Since the position of the T_C anomaly in χ'_{ac} seems to be independent of the frequency of the probing magnetic field, one can exclude a spin-glass ground state. The overall magnetic behaviour is similar to that reported for the RE_3Pt_4 compounds [29] crystallizing with the Pu_3Pd_4 structure type.

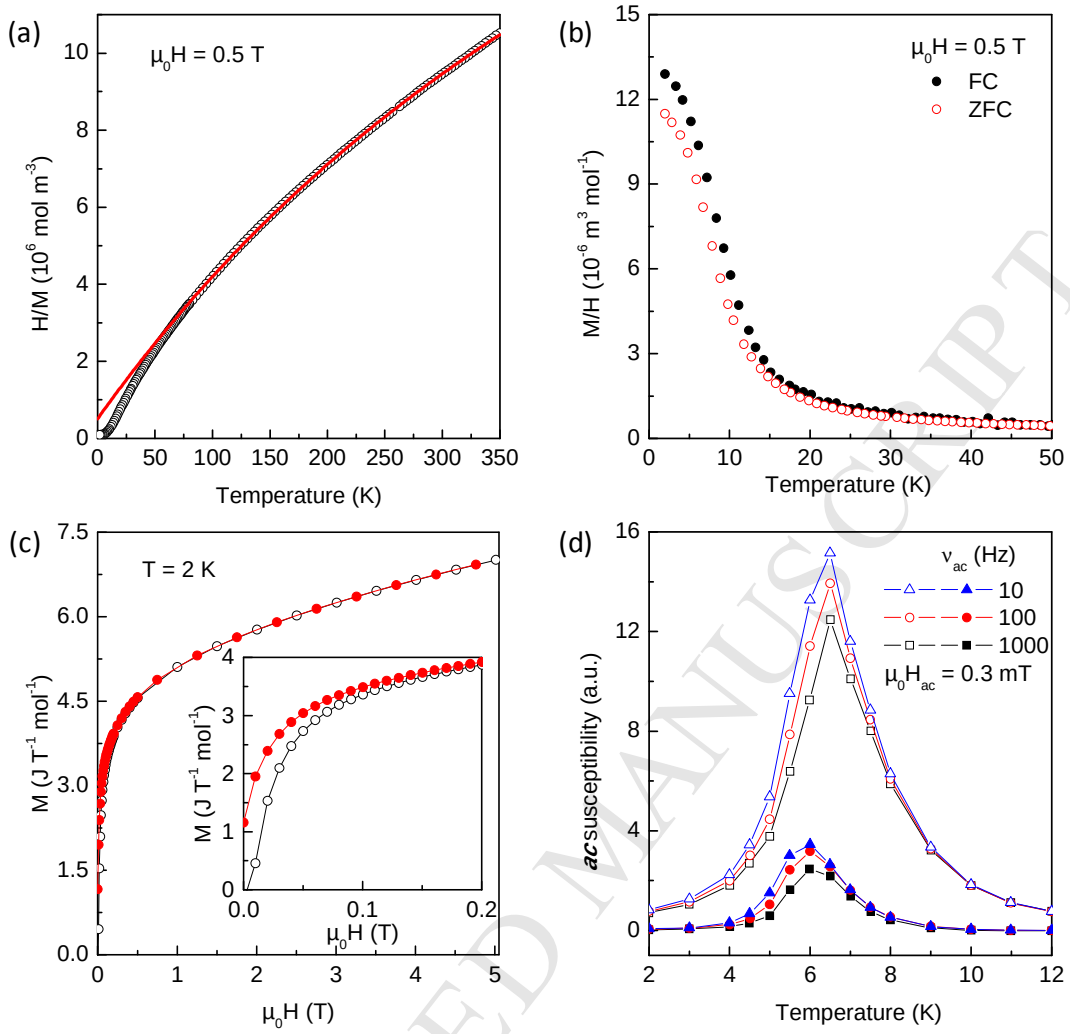

Figure 3. (a) Temperature dependence of the inverse magnetic susceptibility of U_3Pt_4. The red solid line corresponds to the fitting of the modified Curie-Weiss law to the experimental data. (b) Thermal dependence of the magnetic susceptibility measured in the zero-field cooling (ZFC, red) and field cooling (FC, black) regimes. (c) Magnetization isotherm at 2 K measured upon increasing (open black symbols) and decreasing (full red symbols) magnetic field. The inset highlights the low magnetic field behavior. (d) Thermal dependence of the real (open symbols) and imaginary (full symbols) parts of the U_3Pt_4 ac-magnetic susceptibility measured in zero external magnetic field at various frequencies.

D/ Specific heat

Figure 4a presents the specific heat C_p of as-cast Th_3Pt_4 and U_3Pt_4 as a function of temperature. The overall shape of the Cp(T) curves is in line with predictions of the Debye description of lattice vibrations. However, at high temperatures C_p of both compounds tends to saturate at values larger than that expected from the Debye model and hence also from the Dulong-Petit limit (i.e. 7×25 = 175 J K^{-1} mol^{-1}). In the case of Th_3Pt_4 the difference is relatively small and can be ascribed to the specific heat of conduction electrons, completely neglected in the two theoretical approaches mentioned above. In U_3Pt_4 the deviation from the value expected for phonon specific heat is much larger and results most probably from the presence of the uranium *5f* electrons. At high temperature anharmonic vibrations could also play a significant role and yield some non-negligible contribution to the specific heat. In order to verify our predictions and illustrate the approach we have tried to describe the experimental data by the formula [32]:

$$C_p(T) = \gamma T + \frac{1}{(1-\alpha T)} 9rR \left(\frac{T}{\Theta_D}\right)^3 \int_0^{\Theta_D/T} \frac{x^4 e^x}{(e^x-1)^2} dx, \quad (2)$$

in which the first term describes the conduction-electron contribution to the specific heat and the second term is the Debye formula for the phonon specific heat multiplied by an anharmonic term. Fig. 4(a) displays results the least-squares fit of Eq. (2) with r = 7 atoms per formula unit and the universal gas constant R, which yields the Sommerfeld coefficient γ = 9.8(5) mJ K^{-2} mol^{-1}, the anharmonic correction coefficient α = 1.6(1) 10^{-4} K^{-1} and the Debye temperature Θ_D = 170(2) K.

At low temperatures the specific heat of Th_3Pt_4 follows the formula:

$$C_p = \gamma T + \beta T^3 \quad (3)$$

where the second term is the Debye T^3-law (for explanation see *e.g.* [33]). Least squares fits of the experimental data (inset to fig. 4a) yielded γ = 9.9(6) mJ K^{-2} mol^{-1} and β = 2.68(4) mJ K^{-4} mol^{-1}. Θ_D estimated from the latter parameter is equal to 172(1) K. Both the Sommerfeld coefficient and the Debye temperature are from ranges typical for intermetallics and are close to those obtained from eq. (2).

Ferromagnetic ordering observed in magnetic properties at T_C manifests itself as a slightly broadened anomaly in the specific heat of U_3Pt_4 (inset to fig. 4a). Assuming that Th_3Pt_4 is a good phonon reference of the U-based isostructural counterpart, one can estimate the magnetic contribution ΔC_P to the total specific heat of U_3Pt_4 by substracting $C_p(T)$ of Th_3Pt_4. The so-obtained difference is plotted as $\Delta C_P/T$ vs. T in figure 4b. As seen, below the

ordering temperature the anomaly can be described by the formula developed for ferromagnetic spin-waves with an energy gap in the magnon spectrum [33]:

$$\frac{\Delta C_P}{T} = \gamma^* + BT^{1/2}e^{-\Delta/T} \qquad (4)$$

where γ^* = 737(4) mJ mol^{-1} K^{-2} (*i.e.* 246(2) mJ mol$_U^{-1}$ K^{-2}) can be treated as enhancement of the Sommerfeld coefficient coming from the presence of the *5f* electrons of uranium, Δ = 5.4(3) K is the gap in the magnon spectrum and B = 280(2) mJ mol^{-1} K$^{-5/2}$ is a coefficient of proportionality. The value of Δ is close to T_C as observed in various uranium based ferromagnets. The enhanced value of the γ^* coefficient (two orders of magnitude larger than gamma in Th_3Pt_4) suggests a pronounced heavy fermion character of U_3Pt_4.

Taking the theoretical curve (4) up to 2 K and the experimental data above 2 K one can estimate temperature dependence of the magnetic entropy in U_3Pt_4, using the thermodynamic relation:

$$S(T) = \int \frac{C_p(T)}{T} dT \qquad (5)$$

(with the assumption that S(0)=0). The so-obtained S(T) curve is presented in Fig. 4(b) (right axis). As seen the magnetic entropy achieves at the ordering temperature T_C the value of 1/3 of Rln2 per uranium atom, expected for a doublet ground state. Such reduced entropy could be a result of either presence of strong hybridization of the *5f* electrons with conduction band electrons (in line with the enhanced Sommerfeld coefficient in U_3Pt_4) or differences in phonon spectra of U- and Th-based systems, or both effects together.

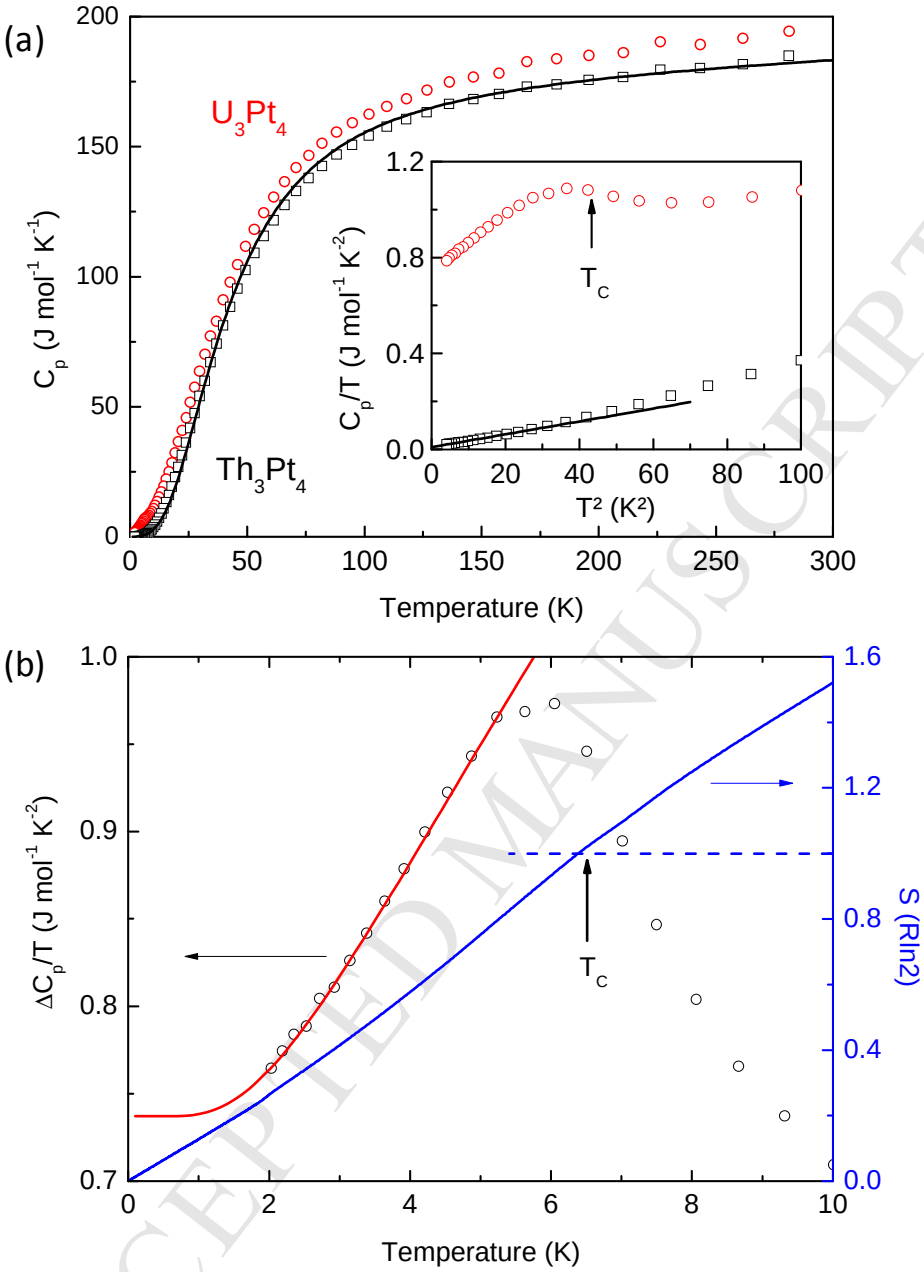

Figure 4. (a) Temperature dependence of the specific heat of U_3Pt_4 (open red circle) and its phonon counterpart Th_3Pt_4 (open black squares). The solid line corresponds to the fit of eq. (2) to the Th_3Pt_4 data. The inset presents the low temperature region of C_P/T as a function of T^2 for both compounds, the solid line being the fit of equation (3) to the Th_3Pt_4 data. (b) Low temperature variation of the 5f electron specific heat (open circles) and corresponding entropy (blue line) normalized to Rln2 values. The red solid line corresponds to the fit of equation (4) to the experimental $\Delta C_P/T$ data. The horizontal dashed blue line indicates the Rln2 value of the entropy.

Conclusions

Our reinvestigation of the U-Pt binary system lead to the discovery of the novel U_3Pt_4 intermetallic phase. Together with the previously mentioned Th_3Pt_4 [9], they crystallize in the trigonal Pu_3Pd_4 structure-type ($R\bar{3}$ space group).

As revealed by the magnetic properties and specific heat measurements, U_3Pt_4 orders ferromagnetically below T_C = 6.5(5) K. Enhanced Sommerfeld coefficient of the specific heat suggests the presence of strong electron interactions and a heavy fermion character of this intermetallics compound. The M/H(T) and C_P(T) curves around the magnetic transition also strongly resembles those reported for the superconducting itinerant ferromagnet UCoGe [34], pushing for further characterization of this platinide. Lower temperature measurements are also desirable on higher purity Th_3Pt_4 to compare it to the isostructural superconductor La_3Pt_4 (Tsc = 0.51 K) [35]. Single crystals are currently under synthesis to perform these investigations.

Acknowledgments

This work is supported in 2015-2017 by the “Finug” CNRS-PAN PICS project (International Program for Scientific Cooperation).

References

[1] J. Gouchi, A. Sumiyama, A. Yamaguchi, G. Motoyama, N. Kimura, E. Yamamoto, Y. Haga, Y. Ōnuki, Unusual pressure evolution of the Meissner and Josephson effects in the heavy-fermion superconductor UPt_3. *Phys. Rev. B,* 93 (2016) 174514.

[2] G. R. Stewart, Z. Fisk, J. O. Willis, J. L. Smith, Possibility of coexistence of bulk superconductivity and spin fluctuations in UPt_3. *Phys. Rev. Lett.*, 52 (1984) 679-682.

[3] B. A. S. Ross, D. E. Peterson, Pt-U (Platinum-Uranium), in *Binary Alloy Phase Diagrams, Second Edition*, T. B. Massalski, Ed.; ASM International, Materials Park, Ohio, volume 3 (1990) 3145-3148.

[4] W.-D. Schneider, C. Laubschat, Actinide-noble-metal systems: an X-ray-photoelectron-spectroscopy study of thorium-platinum, uranium-platinum, and uranium-gold intermetallics. *Phys. Rev. B,* 23 (1981) 997-1005.

[5] J. J. M. Franse, A. A. Menovsky, A. de Visser, P. H. Frings, C. Vettier, Electronic and magnetic properties of uranium-platinum intermetallics compounds. *J. Magn. Magn. Mater*., 70 (1987) 351-358, *and references therein*.

[6] K. Prokeš, T. Fujita, E. Brück, F. R. de Boer, A. A. Menovsky, Magnetic properties of UPt single crystals. *Phys. Rev. B*, 60 (1999) R730-R733.

[7] K. Prokeš, J. C. P. Klaasse, I. H. Hagmusa, A. A. Menovsky, E. H. Brück, F. R. de Boer, T. Fujita, Magnetism in UPt. *J. Phys.:Cond. Matter*, 10 (1998) 10643-10654.

[8] E. D. Bauer, E. J. Freeman, C. Sirvent, M. B. Maple, High-pressure study of ferromagnetic U_xM_{1-x} (M = Pt, Ir) compounds. *J. Phys.:Cond. Matter*, 13 (2001) 5675-5690.

[9] J. R. Thomson, Alloys of thorium with certain transition metals 2. The systems thorium-osmium, thorium-iridium and thorium-platinum. *J. Less-Common Met.*, 6 (1964) 3-10.

[10] R. Gumeniuk, W. Schnelle, U. Burkhardt, H. Borrmann, M. Nicklas, A. Ormeci, M. Kohout, A. Leithe-Jasper, Y. Grin, $ThPt_2$: a new representative of close packed tetragonal structures. *Inorg. Chem.*, 54 (2015) 6338-6346.

[11] J. Rodriguez-Carvajal, Recent developments of the program Fullprof, *Commission on Powder Diffraction (IUCr). Newsletter*, 26 (2001) 12-19.

[12] D.T. Cromer, A. C. Larson, R. B. J. Roof, The crystal structure of Pu_3Pd_4, *Acta Crystallogr. B*, 29 (1973) 564-567.

[13] A. Palenzona, A. Iandelli, The crystal structure and lattice constants of RE_3Pd_4, Y_3Pd_4 and Th_3Pd_4 compounds. *J. Less-Common Met.*, 34 (1974) 121-124.

[14] A. Palenzona, The crystal structure and lattice constants of R_3Pt_4 compounds. *J. Less-Common Met.*, 53 (1977) 133-136.

[15] A. Saccone, M. L. Fornasini, D. Maccio, S. Delfino, Phase equilibria in the Gd-Au system. *Intermetallics*, 4 (1996) 111-119.

[16] A. Saccone, D. Maccio, M. Giovannini, S. Delfino, The praseodymium-gold system. *J. Alloys Compd.*, 247 (1997) 134-140.

[17] A. Saccone, D. Maccio, S. Delfino, R. Ferro, The neodymium-gold phase diagram. *Metall Mater Trans A*, 30 (1999) 1169-1176.

[18] A. Saccone, D. Maccio, S. Delfino, R. Ferro, The phase diagram of the terbium-gold alloy system. *Intermetallics*, 8 (2000) 229-237.

[19] A. Palenzona, S. Cirafici, The Th-Au phase diagram. *J. Less-Common Met.*, 124 (1986) 245- 249.

[20] W. Pitschke, N. Mattern, H. Hermann, Incorporation of microabsorption corrections into Rietveld analysis, *Powder Diffraction*, 8 (1993) 223-228.

[21] W.A. Dollase, Correction of intensities for preferred orientation in powder diffractometry: Application of the March model. *J. Appl. Crystallogr.*, 19 (1986) 267-272.

[22] M. C. Bennet, O. Khalifah, D. A. Sokolov, W.J. Gannon, Y. Yiu, M. S. Kim, C. Henderson, A new unconventional antiferromagnet Yb_3Pt_4. *J. Magn. Magn. Mater*., 321 (2009) 2021-2026.

[23] E. Teatum, K. Gschneidner, J. Waber, *Compilation of calculated data useful in predicting metallurgical behavior of the elements in binary alloy systems*, LA-2345, Los Alamos Scientific Laboratory, 1960.

[24] P. Villars, K. Cenzual, *Pearson's Crystal Data : Crystal Structure Database for Inorganic Compounds,* Release 2009/1, ASM International, Materials Park, Ohio, USA, *and references therein*.

[25] R. G. Jordan, O. Loebich Jr., The magnetic properties of Sm-Pd alloys, *J. Less-Common Met.,* 39 (1975) 55-62.

[26] R. Kuentzler, O. Loebich, Electronic properties and stability of the ordered Pd-Y alloys, *J. Less-Common Met.,* 106 (1985) 335-348.

[27] R. Troć, Z. Gajek, A. Pikul, Dualism of the 5f electrons of the ferromagnetic superconductor UGe_2 as seen in magnetic, transport, and specific-heat data. *Phys. Rev. B,* 86 (2012) 224403.

[28] R. Troć, Z. Gajek, A. Pikul, H. Misiorek, E. Colineau, F. Wastin, Phenomenological crystal-field model of the magnetic and thermal properties of the Kondo-like system UCu_2Si_2. *Phys. Rev. B,* 88 (2013) 024416.

[29] H. Gamari-Seale, J. K. Yakinthos, The magnetic properties of R_3Pt_4 intermetallic compounds, *J. Appl. Phys.,* 50 (1979) 2315-2317.

[30] R. Troć, V. H. Tran, Magnetic properties of UT(Si,Ge) series, *J. Magn. Magn. Mater*., 73 (1988) 389-397.

[31] N. T. Huy, A. de Visser, Ferromagnetic ordering in U(Rh,Co)Ge, *Solid State Commun*., 149 (2009) 703-706.

[32] P. Svoboda, P. Javorský, M. Diviš, V. Sechovský, F. Honda, G. Oomi, A. A. Menovsky, *Phys. Rev. B,* 63 (2001) 212408.

[33] E. S. R. Gopal, *Specific heats at low temperatures*; The International Cryogenic Monograph Series, K. Mendelssohn, K. D. Timmerhaus, eds.; Plenum Press: New York, 1966.

[34] N. T. Huy, A. Gasparini, D. E. de Nijs, Y. Huang, J. C. P. Klaasse, T. Gortenmulder, A. de Visser, A. Hamann, T. Görlach, H. v. Löhneysen, Superconductivity on the border of weak itinerant ferromagnetism in UCoGe, *Phys. Rev. Lett.*, 99 (2007) 067006.

[35] Y. Kawashima, G. Eguchi, S. Yonezawa, Y. Maeno, Superconductivity in La_3Pt_4, *J. Phys. Soc. Jpn.*, 81 (2012) 125001.

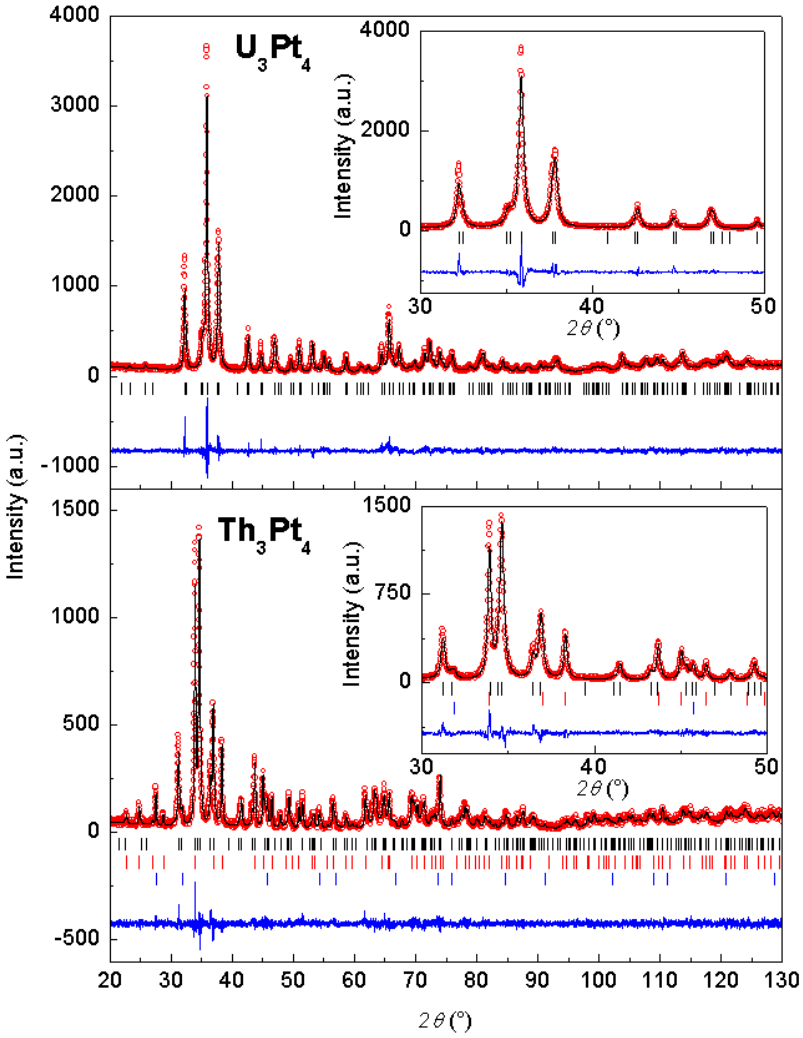

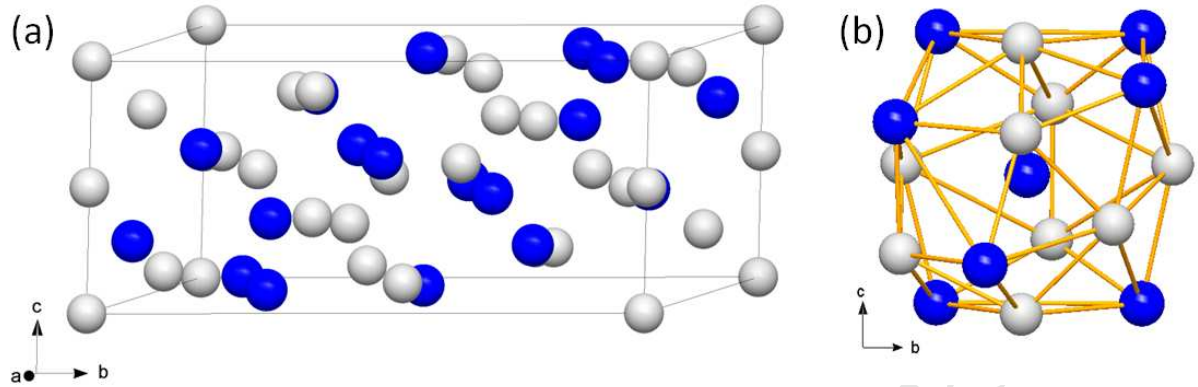

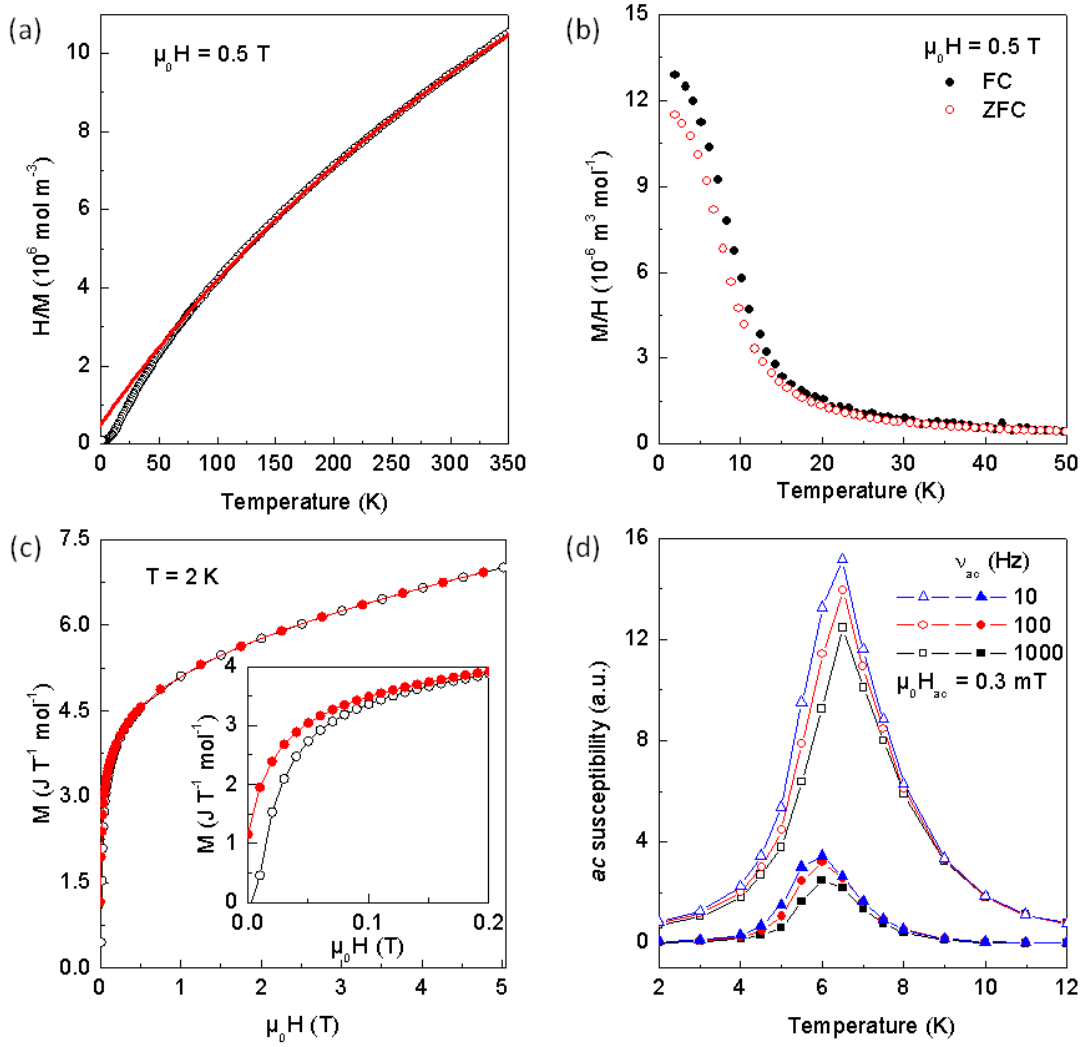
(a)
μ0H = 0.5 T
H/M (10^6 mol m^-3)
Temperature (K)
(b)
μ0H = 0.5 T
FC
ZFC
M/H (10^-6 m^3 mol^-1)
Temperature (K)
(c)
T = 2 K
M (J T^-1 mol^-1)
μ0H (T)
(d)
νac (Hz)
10
100
1000
μ0Hac = 0.3 mT
ac susceptibility (a.u.)
Temperature (K)

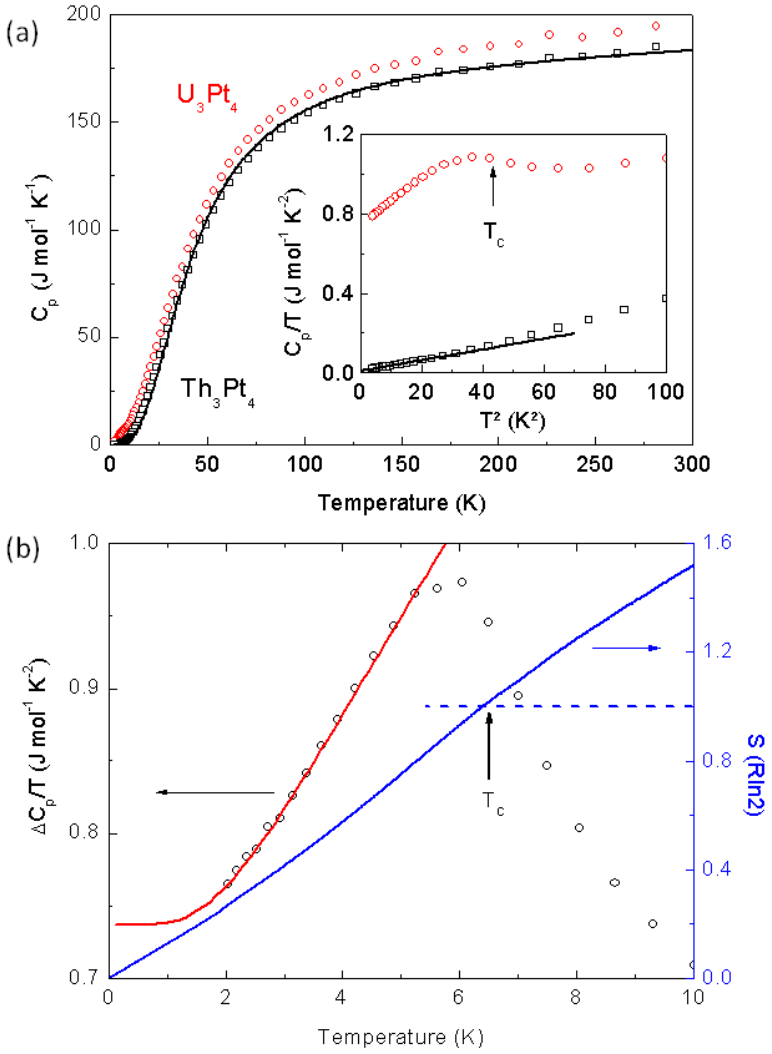
(a)
U3Pt4
Th3Pt4
Cp (J mol-1 K-1)
Temperature (K)
Cp/T (J mol-1 K-2)
T² (K²)
Tc
(b)
ΔCp/T (J mol-1 K-2)
S (Rln2)
Temperature (K)
Tc

- The novel phases A_3Pt_4 (A = Th, U) crystallizes with the Pu_3Pd_4 structure-type
- U_3Pt_4 orders ferromagnetically below T_C = 6.5(10) K
- U_3Pt_4 exhibits a heavy fermion behaviour (γ = 246(2) mJ mol_U^{-1} K^{-2})